Chinese Medical Journal®

Development of a radiomics model to discriminate ammonium urate stones from uric acid stones *in vivo*: A remedy for the diagnostic pitfall of dual-energy computed tomography

Junjiong Zheng[1], Jie Zhang[1], Jinhua Cai[2], Yuhui Yao[1], Sihong Lu[1], Zhuo Wu[3], Zhaoxi Cai[3], Aierken Tuerxun[4], Jesur Batur[4], Jian Huang[1], Jianqiu Kong[1], Tianxin Lin[1]

[1]Department of Urology, Sun Yat-Sen Memorial Hospital, Sun Yat-Sen University, Guangdong Provincial Key Laboratory of Malignant Tumor Epigenetics and Gene Regulation, Guangdong Provincial Clinical Research Center for Urological Diseases, Guangzhou, Guangdong 510120, China;
[2]Department of Neurology, Sun Yat-Sen Memorial Hospital, Sun Yat-Sen University, Guangzhou, Guangdong 510120, China;
[3]Department of Radiology, Sun Yat-Sen Memorial Hospital, Sun Yat-Sen University, Guangzhou, Guangdong 510120, China;
[4]Department of Urology, The First People's Hospital of Kashgar Prefecture, Kashgar, Xinjiang 844000, China.

Abstract

Background: Dual-energy computed tomography (DECT) is purported to accurately distinguish uric acid stones from non-uric acid stones. However, whether DECT can accurately discriminate ammonium urate stones from uric acid stones remains unknown. Therefore, we aimed to explore whether they can be accurately identified by DECT and to develop a radiomics model to assist in distinguishing them.

Methods: This research included two steps. For the first purpose to evaluate the accuracy of DECT in the diagnosis of uric acid stones, 178 urolithiasis patients who underwent preoperative DECT between September 2016 and December 2019 were enrolled. For model construction, 93, 40, and 109 eligible urolithiasis patients treated between February 2013 and October 2022 were assigned to the training, internal validation, and external validation sets, respectively. Radiomics features were extracted from non-contrast CT images, and the least absolute shrinkage and selection operator (LASSO) algorithm was used to develop a radiomics signature. Then, a radiomics model incorporating the radiomics signature and clinical predictors was constructed. The performance of the model (discrimination, calibration, and clinical usefulness) was evaluated.

Results: When patients with ammonium urate stones were included in the analysis, the accuracy of DECT in the diagnosis of uric acid stones was significantly decreased. Sixty-two percent of ammonium urate stones were mistakenly diagnosed as uric acid stones by DECT. A radiomics model incorporating the radiomics signature, urine pH value, and urine white blood cell count was constructed. The model achieved good calibration and discrimination {area under the receiver operating characteristic curve (AUC; 95% confidence interval [CI]), 0.944 (0.899–0.989)}, which was internally and externally validated with AUCs of 0.895 (95% CI, 0.796–0.995) and 0.870 (95% CI, 0.769–0.972), respectively. Decision curve analysis revealed the clinical usefulness of the model.

Conclusions: DECT cannot accurately differentiate ammonium urate stones from uric acid stones. Our proposed radiomics model can serve as a complementary diagnostic tool for distinguishing them *in vivo*.

Keywords: Ammonium urate; Dual-energy scanned projection radiography; Radiomics; Uric acid; Urolithiasis

Introduction

Urolithiasis is one of the most common benign diseases of the urinary system. It is a worldwide health problem that has caused a tremendous economic burden to public health systems.[1,2] The prevalence and incidence of urolithiasis have been reported to be increasing over the past several decades.[2] A population-based study showed that the global incidence of urolithiasis in 2019 was 48.57% higher than that in 1990, and the incidence of symptomatic kidney stones that require treatment is also increasing.[3,4]

Therapeutic regimen options vary between patients with stones of different compositions. In addition, knowledge

Access this article online

Quick Response Code:

Website: www.cmj.org

DOI: 10.1097/CM9.0000000000002866

Junjiong Zheng, Jie Zhang, and Jinhua Cai contributed equally to this work.

Correspondence to: Prof. Tianxin Lin, Department of Urology, Sun Yat-Sen Memorial Hospital, Sun Yat-Sen University, No. 107 Yan Jiang West Road, Guangzhou, Guangdong 510120, China
E-Mail: lintx@mail.sysu.edu.cn;
Dr. Jianqiu Kong, Department of Urology, Sun Yat-Sen Memorial Hospital, Sun Yat-Sen University, No. 107 Yan Jiang West Road, Guangzhou, Guangdong 510120, China
E-Mail: kongjq5@mail.sysu.edu.cn

Chinese Medical Journal 2024;137(9)
Received: 05-06-2023; **Online:** 23-11-2023 **Edited by:** Yuanyuan Ji

of stone composition helps to identify appropriate medical and lifestyle interventions to prevent stone recurrence.[5–7] Therefore, clinical guidelines recommend that stone composition analysis should be performed for urolithiasis patients.[8,9] Currently, infrared spectroscopy is the most commonly used method for stone composition analysis. However, it can only be carried out *in vitro* after extracting stone specimens via surgery or stone expulsion. If stone composition can be accurately predicted before treatment, it may aid in clinical decision-making and help to improve patient outcomes.

Dual-energy computed tomography (DECT) has good application prospects in the preoperative prediction of stone composition. On DECT imaging, materials with low atomic numbers have small attenuation differences between the two energy levels, while those with high atomic numbers have larger attenuation differences[10]; this is the principle behind the theory that DECT can predict stone composition. Uric acid stones are composed of elements with low atomic numbers, i.e., carbon, hydrogen, nitrogen, and oxygen, while calcium-based stones contain elements, such as calcium and phosphorus, with high atomic numbers. Therefore, DECT can accurately distinguish uric acid from non-uric acid stones.[10,11] Recently, a meta-analysis indicated that the pooled diagnostic sensitivity and specificity of DECT were 0.880 and 0.980, respectively.[12] Notably, uric acid and ammonium urate have the same composition of atomic species (chemical structural formulas are shown in Supplementary Figure 1, http://links.lww.com/CM9/B751). Therefore, we hypothesized that DECT may be unable to accurately distinguish ammonium urate stones from uric acid stones based on the above principle. Whether DECT can accurately discriminate the two types of stones remains unknown, which is well worth investigating.

Ammonium urate stones are rare in economically developed areas, accounting for 0.38–8.7%,[13–19] while they are common in economically underdeveloped areas, accounting for over 28.2%.[20–23] The physicochemical properties of uric acid and ammonium urate stones are very different. Uric acid stones are non-infected stones that are formed when urine pH is less than 5.5.[24] They are stable in an acidic environment and dissolve during urine alkalization. Ammonium urate stones are classified as infection stones, which are presumed to be associated with urinary tract infections caused by urease-producing gram-negative organisms.[25,26] Ammonium urate stones are formed when the urine pH is approximately 6.3 and are stable in an alkaline environment.[27,28] Thus, there are considerable differences in treatment and preventive strategies. For ammonium urate stones, using antibiotics during the perioperative period is necessary since infected stones have a higher risk of postoperative infectious complications. Furthermore, the complete removal of stones without residual disease is critical and plays an important role in the prevention of recurrence.[29,30] In contrast, uric acid stones are capable of chemolysis and can be treated with alkaline drugs to avoid invasive stone removal when appropriate. In addition, the treatment of hyperuricemia and alkalized urine are important strategies to prevent recurrence.[31,32] Therefore, it is of great clinical significance to accurately distinguish between these two types of stones at the time of diagnosis.

Radiomics is a promising approach for extracting high-throughput quantitative image features from medical images and applying useful features within clinical decision support systems.[33] Although radiomics is mainly applied in the field of oncology,[33–35] our previous multicentric study demonstrated that radiomics can also be applied to urinary stone disease.[36] This provides novel insights into solving some relevant clinical issues in urolithiasis.

Therefore, our study aimed to explore whether DECT can accurately distinguish ammonium urate stones from uric acid stones. In addition, we attempted to develop a radiomics model based on non-contrast CT images and urinalysis results for preoperatively discriminating the two types of stones.

Methods

Patients

This retrospective study was approved by the Ethics Review Board at the First People's Hospital of Kashgar Prefecture and the Sun Yat-Sen Memorial Hospital (Nos. FPHKP-KSY-2021028 and SYSEC-KY-KS-2020-126), and the need for informed consent was waived. The flowcharts and workflow of the study are shown in Figure 1. Our research included two steps. The first step was to evaluate the accuracy of DECT in the diagnosis of uric acid stones. For this purpose, 178 eligible patients with urinary stones treated from September 2016 to December 2019 in the First People's Hospital of Kashgar Prefecture were enrolled. These patients underwent DECT before surgery, and stones removed from these patients underwent stone component analysis. The second step was to construct a radiomics model for individualized preoperative differentiation of uric acid stones from ammonium urate stones. We included 133 eligible urolithiasis patients treated from February 2013 to December 2019 in the First People's Hospital of Kashgar Prefecture. These patients fulfilled the following inclusion criteria: (1) diagnosed with urolithiasis; (2) underwent surgery to remove the urinary stone, which was analyzed for stone composition; (3) predominant stone composition of uric acid or ammonium urate; and (4) non-contrast CT (single-energy CT or DECT), urinalysis, and urine culture performed before surgery. We randomly divided the patients into a training set and an internal validation set at a ratio of 7:3 using computer-generated random numbers. In addition, 109 urolithiasis patients treated from July 2016 to October 2022 in the Sun Yat-Sen Memorial Hospital were used as the external validation set. It has been proposed that for multivariate logistic regression, a minimum of 10 to 15 observations per predictor variable is required to produce reasonably stable estimates.[37] In our study, we obtained more than 15 observations per predictor variable in the training set.

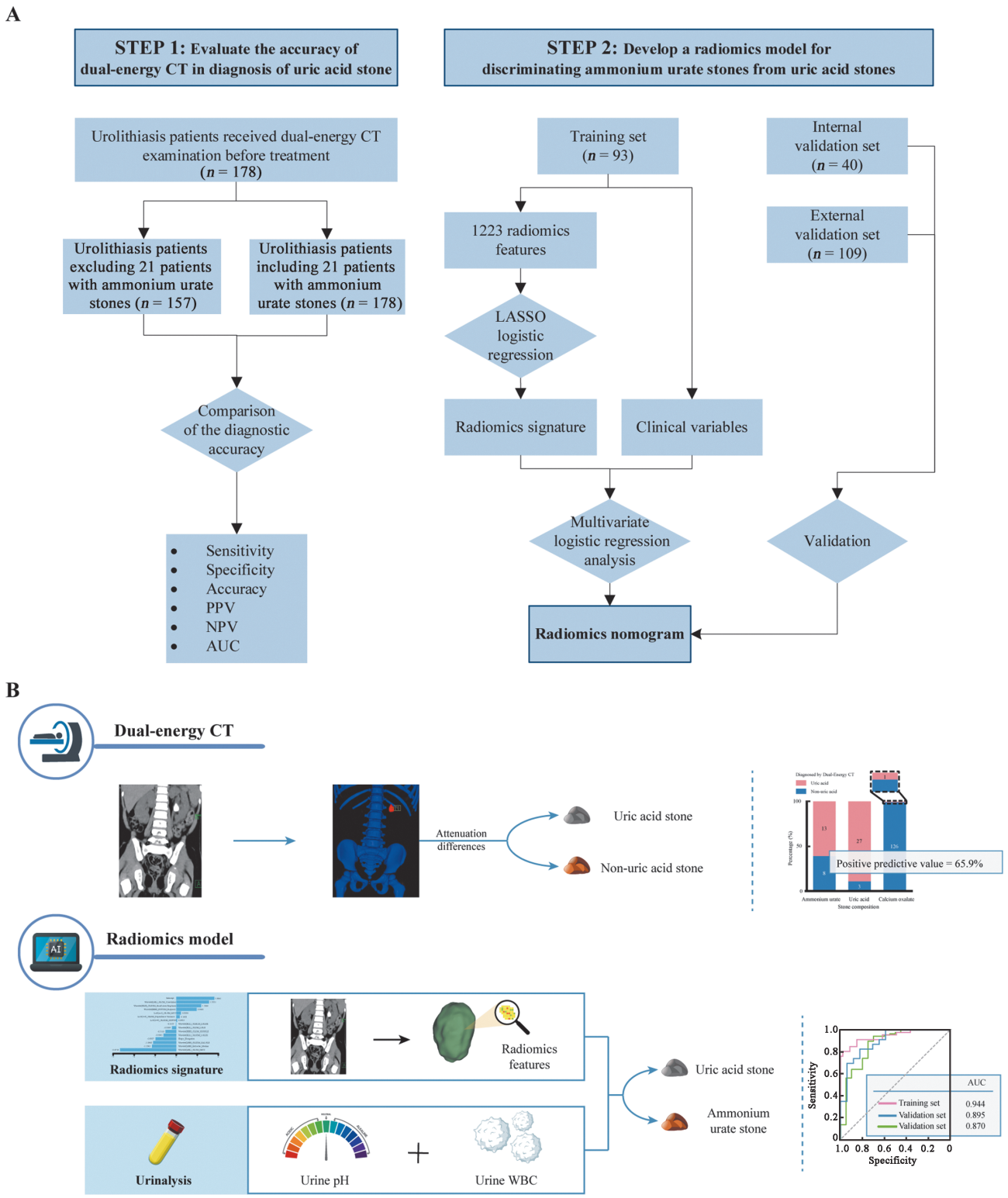

Figure 1: Flowcharts and workflow of the study. (A) Study flowcharts. (B) Study workflow. AUC: Area under the receiver operating characteristic curve; CT: Computed tomography; NPV: Negative predictive value; PPV: Positive predictive value; LASSO: Least absolute shrinkage and selection operator; WBC: White blood cell.

Baseline clinical data, including age, sex, and results of routine urinalysis tests and urine cultures, were obtained from medical records. The DECT images and non-enhanced CT images were reviewed by two experienced radiologists, and the data obtained from the CT images were recorded, including the location and number of stones and the prediction results of stone composition via DECT. Any differences were resolved by negotiation. In this study, Fourier transform infrared spectroscopy was used to assess the composition of stones. The composition

was considered predominant if it exceeded 50% of the total composition of the stones. The image processing and interpretation of DECT are described in the Supplementary Methods, http://links.lww.com/CM9/B751. The DECT and non-enhanced CT image acquisition settings are listed in Supplementary Table 1, http://links.lww.com/CM9/B751.

Radiomics procedure

All patients underwent non-contrast CT scans before stone removal. The CT images (Digital Imaging and Communications in Medicine [DICOM] format) were retrieved for radiomics analysis. The radiomics analysis procedure for urinary stones previously established by our research team was used in this study.[36] The reproducibility of this method has been previously confirmed. Detailed information about the radiomics procedure can be found in our previous study.[36] Briefly, volumes of interest (VOIs) of the urinary stone were semiautomatically segmented using the thresholding segmentation method implemented in the publicly available 3D Slicer software (version 4.10.0, http://www.slicer.org). Then, 1223 radiomics features were extracted from each VOI, which were normalized to a range from 0 to 1 using linear transformation for the subsequent analysis. Radiomics feature extraction was performed using the *PyRadiomics* platform (version 3.0) implanted in Python software (version 3.7.4, http://www.python.org),[38] and the extracted features are presented in Supplementary Table 2, http://links.lww.com/CM9/B751.

Radiomics signature construction and performance evaluation

The least absolute shrinkage and selection operator (LASSO) algorithm is a powerful machine learning method for variable selection. In the training set, we used the LASSO logistic regression algorithm to select the most useful prediction features. Then, a radiomics signature was constructed based on the selected features, which was represented as a radiomics score. The radiomics score of each patient was calculated as a linear combination of selected features, which were weighted by their corresponding LASSO coefficients.[39]

The Mann–Whitney *U* test was utilized to evaluate whether there was a significant difference in radiomics scores between patients with uric acid stones and patients with ammonium urate stones. In addition, the discrimination of the radiomics signature was quantified by the area under the receiver operating characteristic (ROC) curve (AUC) in the training set and validation sets, respectively. An optimism-corrected AUC was also calculated by the bootstrapping method (2000 bootstrap resamples) to obtain stable optimism-corrected estimates.[40] Furthermore, stratified analyses were performed within various subgroups of the patients in the combined training set and two validation sets.

Radiomics model construction and performance evaluation

In the training set, a multivariate logistic regression algorithm was used to develop a radiomics model. The likelihood ratio test and the stopping rule of the Akaike information criterion (AIC) were used to identify the independent predictors among the radiomics score and other candidate clinical variables for discriminating uric acid stones from ammonium urate stones by backward stepwise selection. Then, a radiomics model was constructed, which was graphically presented as a nomogram. Collinearity diagnostics were evaluated by calculating the variance inflation factor (VIF). The performance of the model was assessed in terms of discrimination and calibration in the training set and validated in the validation sets. AUCs (including optimism-corrected AUCs) and calibration curves were used to evaluate the discriminative ability and calibration of the model, respectively. In addition, the Hosmer–Lemeshow test was used to evaluate the goodness-of-fit of the model.[41]

Clinical usefulness of the radiomics model

By calculating the net benefit under different threshold probabilities, decision curve analysis (DCA) was performed to determine the clinical usefulness of the radiomics model.[42] In addition, ROC analyses were used in the combined training set and two validation sets to compare the discrimination efficacy between the radiomics model and the variables incorporated in the nomogram alone.

Statistical analysis

Continuous variables were summarized as the mean ± standard deviation when the assumption of normal distribution was satisfied, and the *t*-tests were used to compare the means. Data were expressed as the median and interquartile range (IQR) when variables were not normally distributed, and a non-parametric test was used to compare the medians. Categorical variables were presented as percentages. All statistical analyses were conducted using R software (R Statistical Computing Base, version 4.0.4, https://www.r-project.org/). The R packages used in this study are listed in Supplementary Table 3, http://links.lww.com/CM9/B751. Detailed information about the LASSO algorithm and DCA are available in the Supplementary Methods, http://links.lww.com/CM9/B751. All statistical tests were two-tailed, and a *P*-value of <0.050 was considered statistically significant.

Results

Patient clinical characteristics

Supplementary Table 4 (http://links.lww.com/CM9/B751) lists the clinical baseline characteristics of patients with urinary calculi who underwent DECT. Among them, there were 30 patients with uric acid stones, 21 patients with ammonium urate stones, and 127 patients with calcium oxalate stones. The clinical baseline characteristics of patients enrolled to develop and validate the radiomics model are summarized in Supplementary Table 5, http://links.lww.com/CM9/B751.

Accuracy of DECT in the diagnosis of uric acid stones

In the patients who underwent DECT, we attempted to evaluate the accuracy of DECT in the diagnosis of uric

acid stones. When patients with ammonium urate stones were not included in the analysis, the diagnostic sensitivity, specificity, and accuracy of DECT were 90.0%, 99.2%, and 97.5%, respectively [Figure 2A], and the AUC was 0.946 (95% confidence interval [CI], 0.891–1.000; Figure 2B). However, among all 178 patients, the sensitivity, specificity, and accuracy were 90.0%, 90.5%, and 90.4%, respectively [Figure 2C]. Moreover, the AUC decreased to 0.903 (95% CI, 0.843–0.962; Figure 2D). Figure 2E further presents an overview of the DECT diagnosis results. A total of 62% of ammonium urate stones were mistakenly diagnosed as uric acid stones by DECT. Thus, DECT is unable to accurately distinguish uric acid and ammonium urate stones.

Radiomics signature construction and performance evaluation

In the training set, 14 uric acid stone-related radiomics features with non-zero coefficients were screened via the LASSO logistic regression algorithm [Figures 3A, B]. The selected radiomics features and their corresponding coefficients are shown in Figure 3C.

In the training set, there was a significant difference in radiomics scores between patients with ammonium urate stones and those with uric acid stones, which was confirmed in the validation sets [Figure 4A]. Moreover, as shown in Supplementary Table 6, http://links.lww.com/CM9/B751, significant differences were found in the stratified analyses for various stratified variables. The AUC of the radiomics signature was 0.924 (95% CI, 0.869–0.978) in the training set, and the optimism-corrected AUC of the radiomics signature was 0.848. The radiomics signature also yielded AUCs of 0.875 (95% CI, 0.768–0.982) and 0.837 (95% CI, 0.726–0.947) in the internal and external validation sets, respectively [Figure 4B]. According to the maximum Youden index in the training set, the optimal radiomics score cutoff value was −0.031. The waterfall plot shows the urinary stone types and corresponding radiomics scores of all enrolled patients, with the dividing line drawn at the cutoff value [Figure 4C].

Radiomics model construction and performance evaluation

According to the multivariate logistic regression algorithm, the radiomics score, urine pH value, and urine white blood cell (WBC) count were identified as independent predictors of uric acid stones [Table 1]. In terms of the collinearity diagnostics, the VIFs of the candidate predictors ranged from 1.039 to 1.255, suggesting that

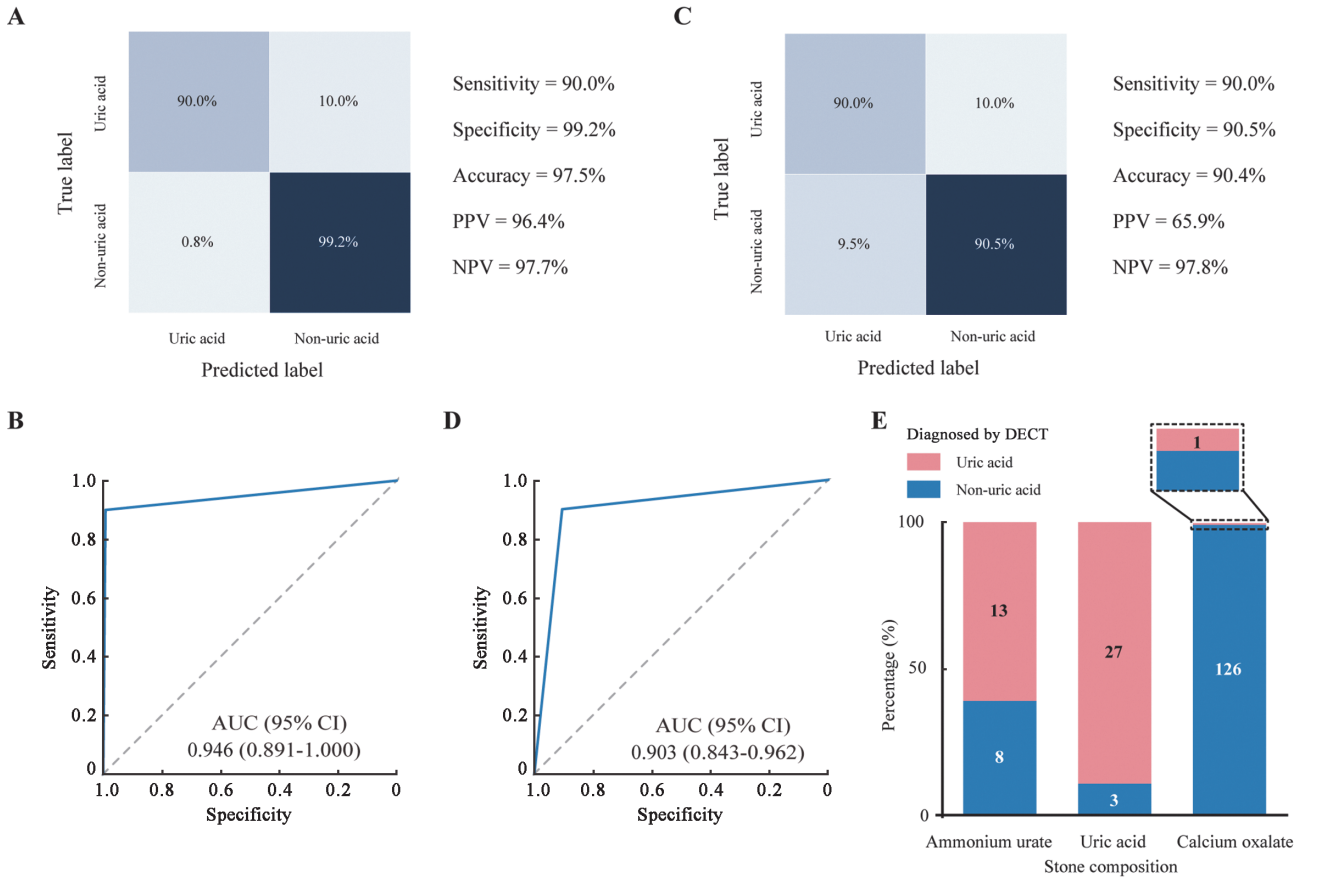

Figure 2: Accuracy of DECT in the diagnosis of uric acid stones. (A, B) Confusion matrix (A) and ROC curve (B) of DECT in the diagnosis of uric acid stones when patients with ammonium urate stones were excluded from the analysis. (C, D) Confusion matrix (C) and ROC curve (D) of DECT in the diagnosis of uric acid stones when patients with ammonium urate stones were included in the analysis. (E) Histogram presenting the overview of DECT diagnosis results in the whole cohort. AUC: Area under the receiver operating characteristic curve; CI: Confidence interval; DECT: Dual-energy computed tomography; NPV: Negative predictive value; PPV: Positive predictive value; ROC: Receiver operating characteristic.

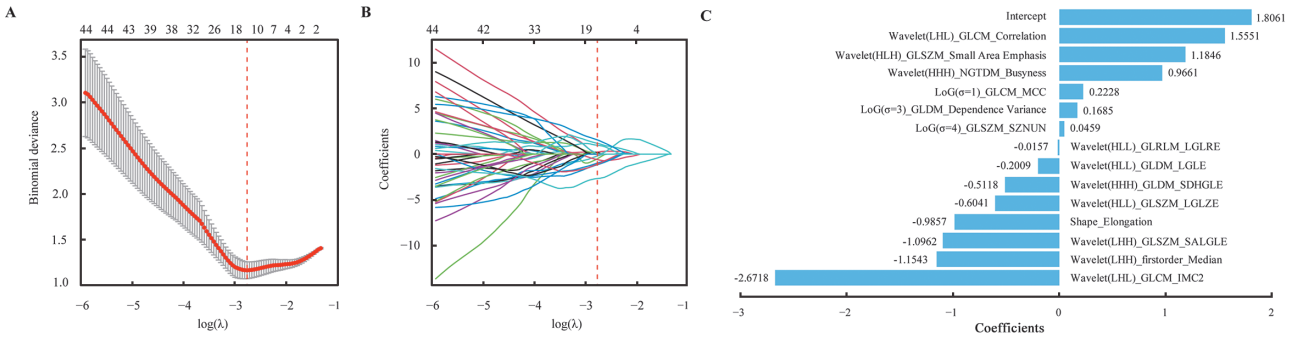

Figure 3: Radiomics signature construction. (A) Tuning parameter selection (λ) with 10-fold cross-validation in the LASSO logistic regression model. The dotted vertical line is drawn at the optimal λ value by minimum criteria, which is 0.063 with log (λ) = −2.761. (B) LASSO coefficient profiles of the candidate variables. (C) The histogram presents the 14 selected features and their corresponding coefficients in the radiomics signature. Features are all shown in the format of "filter_feature class_feature name". Refer to Supplementary Table 2, http://links.lww.com/CM9/B751for the full feature names of the abbreviations. LASSO: Least absolute shrinkage and selection operator.

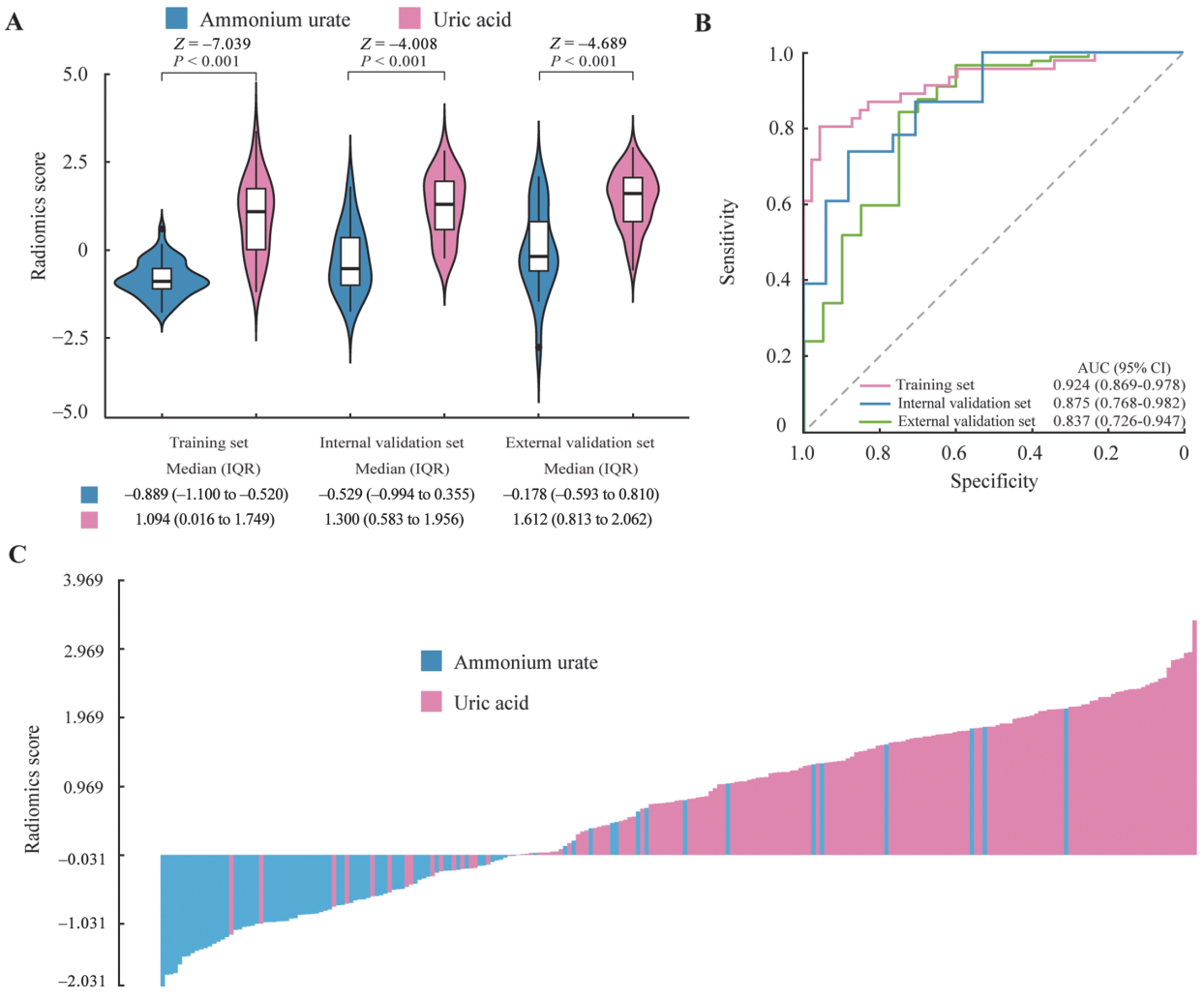

Figure 4: Performance of the radiomics signature. (A) Boxplots of the radiomics score. (B) ROC curves of the radiomics signature. (C) Waterfall plot shows the distribution of radiomics score and stone composition in the combined training set and two validation sets. AUC: Area under the receiver operating characteristic curve; CI: Confidence interval; IQR: Interquartile range; ROC: Receiver operating characteristic.

there was no collinearity. Hence, a radiomics model was constructed by incorporating the above three independent predictors, and the user-friendly nomogram is provided in Figure 5A.

Table 1: Logistic regression analysis of the radiomics score and clinical candidate predictors in the training set.

			Multivariate logistic regression			
	Univariate logistic regression		Radiomics model		Clinical model	
Variables	OR (95% CI)	*P*-value	OR (95% CI)	*P*-value	OR (95% CI)	*P*-value
Radiomics score (per 0.1 increase)	1.304 (1.187–1.486)	<0.001	1.270 (1.163–1.436)	<0.001		
Urine pH	0.255 (0.099–0.580)	0.002	0.373 (0.093–1.391)	0.149	0.277 (0.110–0.631)	0.004
Urine WBC count per microliter (<100 *vs.* ≥100)	0.208 (0.081–0.503)	<0.001	0.221 (0.045–0.948)	0.048	0.207 (0.074–0.536)	0.002
Urine nitrite (negative *vs.* positive)	0.339 (0.124–0.865)	0.028				
Urine culture (negative *vs.* positive)	2.040 (0.825–5.257)	0.128				

CI: Confidence interval; OR: Odds ratio; WBC: White blood cell.

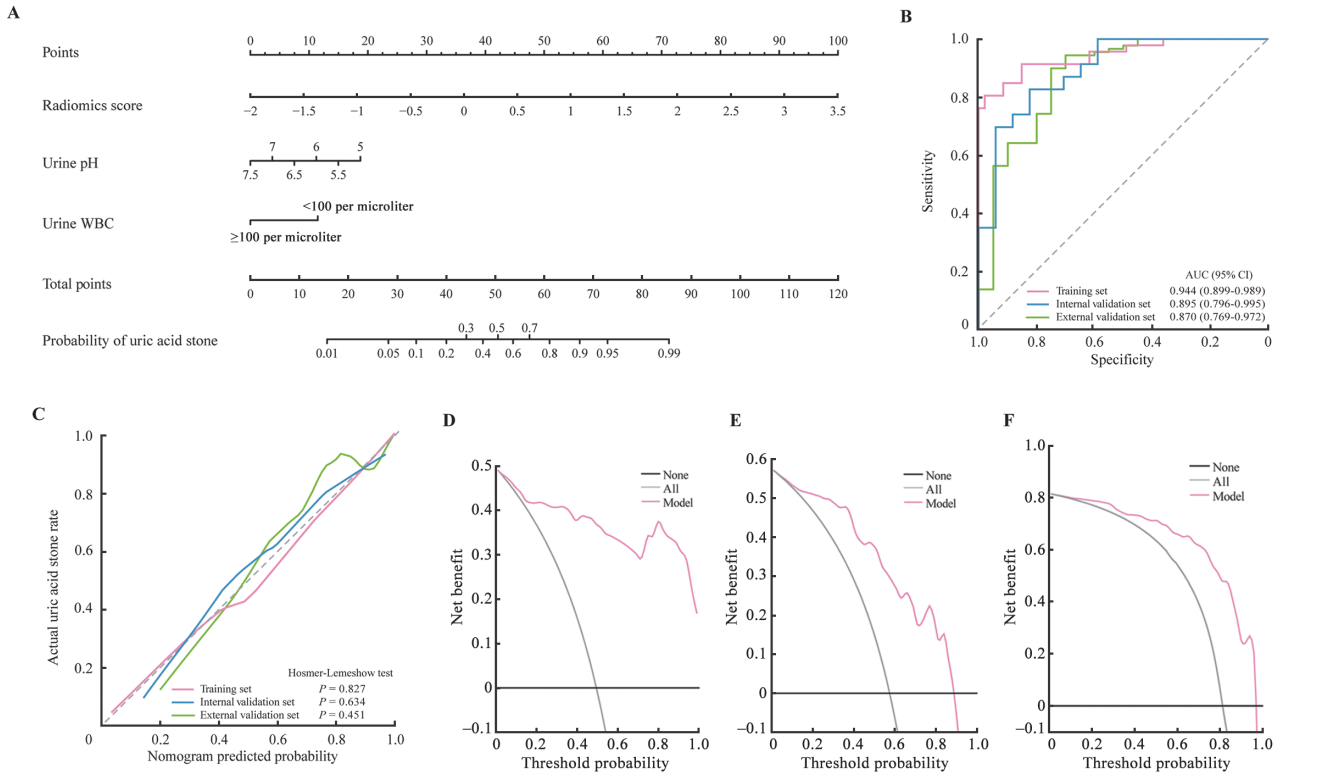

Figure 5: Performance of the radiomics model. (A) The nomogram was constructed based on the radiomics model. (B) ROC curves of the radiomics model. (C) Calibration curve of the radiomics model. The dotted line represents perfect prediction. The calibration curve (solid line) has a closer fit to the dotted line, indicating a better calibration. (D–F) DCA curves of the radiomics model in the training set (D), internal validation set (E), and external validation set (F). The decision curve presents the net benefit *vs.* the threshold probability. The red line refers to the radiomics model. The gray line represents the hypothesis that all patients suffered from uric acid stones, while the black line represents the assumption that no patients had uric acid stones. CI: Confidence interval; DCA: Decision curve analysis; ROC: Receiver operating characteristic.

The radiomics model yielded an AUC of 0.944 (95% CI, 0.899–0.989; Figure 5B) in the training set and an optimism-corrected AUC of 0.889, indicating favorable discrimination. It was validated in the internal and external validation sets, with AUCs of 0.895 (95% CI, 0.796–0.995) and 0.870 (95% CI, 0.769–0.972; Figure 5B), respectively. The calibration curves for the training and validation sets both showed good calibration of the radiomics model [Figure 5C]. The *P*-values obtained by the Hosmer–Lemeshow tests were 0.827 (χ^2 = 4.320), 0.634 (χ^2 = 6.116), and 0.451 (χ^2 = 7.819) in the training set, internal validation set, and external validation set, respectively, indicating no departure from a good fit.

Clinical usefulness of the radiomics model

In the training set and the two validation sets, DCA showed that using our proposed radiomics model to differentiate uric acid stones from ammonium urate stones had more net benefit than the "treat all" or "treat none" strategy at a wide threshold probability, representing the clinical usefulness of the model [Figures 5D–F].

As shown in Supplementary Figure 2, http://links.lww.com/CM9/B751, the ROC curves indicated that the radiomics model had better discriminatory accuracy than either the radiomics signature, urine pH, or urine WBC count alone. A clinical model containing only clinical predictors (i.e., urine pH and urine WBC count)

was constructed by using a multivariate logistic regression algorithm [Table 1]. The performance of the radiomics model was also significantly better than that of the clinical model [Supplementary Figure 2, http://links.lww.com/CM9/B751], indicating that the radiomics signature enhances the predictive value of the clinical model.

Supplementary Figure 3 (http://links.lww.com/CM9/B751) intuitively shows the specific situation of DECT and the radiomics model to distinguish uric acid and ammonium urate stones. We found that only 3 of the 30 uric acid stones were mistakenly diagnosed as non-uric acid stones by DECT, but 13 of the 21 ammonium urate stones were mistakenly diagnosed as uric acid stones. Encouragingly, 88% (14/16) of the misdiagnosed stones were reclassified correctly by using the radiomics model. In addition, net reclassification improvement (NRI) and integrated discrimination improvement (IDI) indices were also calculated.[43] Both the NRI and IDI indices (overall category-based NRI = 0.524, P <0.001; IDI = 0.597, P <0.001) indicated that the radiomics model significantly improved the diagnostic accuracy compared to that of DECT.

The recommended diagnostic workflow for the individualized use of our proposed radiomics model is presented in Supplementary Figure 4, http://links.lww.com/CM9/B751. For patients diagnosed with uric acid stones by DECT, the radiomics model should be used further to avoid misdiagnosis.

Discussion

Our study demonstrated that DECT is unable to accurately distinguish ammonium urate stones from uric acid stones based on a retrospective cohort. For this reason, we further developed a radiomics model incorporating the CT-based radiomics signature, urine pH, and urine WBC count for individualized discrimination *in vivo*. The proposed non-invasive model had favorable prediction capability with internal and external validation, which may aid in clinical decision-making for urolithiasis patients.

The physical and chemical properties, treatment strategies, and preventive measures of ammonium urate and uric acid stones are very different. Hence, it is important to accurately distinguish them before treatment, especially in areas with a high incidence of ammonium urate stones. As stone composition is usually unknown before treatment, researchers have attempted to find novel approaches for the preoperative prediction of urinary stone composition *in vivo*. Uric acid and ammonium urate calculi are both radiolucent on X-ray, and so plain abdominal X-ray is also unable to discriminate them. DECT is an imaging technique that acquires data at two different energy settings, and the composition of the materials imaged can be predicted based on the attenuation difference values between the two energy levels.[10,12] Many studies have shown that DECT can accurately distinguish uric acid from non-uric acid stones.[12] However, none of these studies included ammonium urate stone patients, and so we could not confirm whether DECT can discriminate them from uric acid stone patients. In our study, 21 (11.8%) patients with ammonium urate stones were enrolled. We found that it was difficult to differentiate ammonium urate stones from uric acid stones by using DECT. This informs clinicians that the DECT diagnostic results should be treated with considerable caution in clinical practice, especially in areas with a high incidence of ammonium urate stones. As such, there is a critical need to further develop a complementary diagnostic tool to avoid misdiagnosis.

Radiomics is a promising technique that may potentially facilitate precision medicine.[33] High-dimensional radiomics features can be extracted via the radiomics approach to provide comprehensive information about the target lesions, which in turn improves clinical decision support systems.[33,44] Previously, we demonstrated that CT-based radiomics features can reflect the heterogeneity of urinary stones and can be used to predict the probability of struvite and carbonate apatite stones.[36] In this study, we successfully constructed a CT-based radiomics signature for differentiating ammonium urate stones from uric acid stones. This further expands the application of radiomics in patients with urolithiasis. Additionally, a radiomics model incorporating the radiomics signature and clinical predictors was developed. Among the candidate clinical variables, urine pH and urine WBC count were identified as independent predictors, with odds ratios of 0.373 and 0.221, respectively. This suggests that the lower the urine pH is, the greater the possibility of uric acid stones will be, which is consistent with the physicochemical features of uric acid and ammonium urate stones.[24,27,28] In addition, because ammonium urate stones are infection stones, patients with ammonium urate stones often have urinary tract infections, which are manifested in elevated urine WBC counts.[25,26] This supports the plausibility of our findings.

Our study demonstrated that DECT cannot accurately discriminate ammonium urate stones from uric acid stones, revealing a diagnostic pitfall of DECT. Therefore, we developed a radiomics model for individualized preoperative differentiation. The predictors incorporated in the proposed model are available from routine CT examination and urinalysis. Thus, our model can serve as a non-invasive tool without any extra tests or costs. Our study provides a remedy for the diagnostic pitfall of DECT, which could reduce the rate of missed diagnosis in ammonium urate stones. This may optimize disease management in urolithiasis and improve patient prognosis.

Despite these strengths, our study had several limitations. The patients who underwent DECT enrolled in our study were all from a single center. More multicenter data are required to verify our findings. Similarly, although the radiomics model was internally and externally validated, further prospective validation is warranted to confirm the robustness of our proposed model. In addition, due to the retrospective design and strict inclusion criteria, potential selection biases might have occurred in our study. Only patients with uric acid or ammonium urate stones were included for model construction and

validation. This may limit the application scope of our radiomics model. Based on the strengths and limitations of our study, we envision the following directions guiding the next step of the research, namely conducting a prospective validation study, applying artificial intelligence algorithms to enhance the predictive value of our model, and enrolling urolithiasis patients with various compositions to expand the application scope of our model.

In conclusion, our study revealed that DECT cannot accurately differentiate ammonium urate stones from uric acid stones. To address this issue, we further constructed and validated a radiomics model as a complementary diagnostic tool for distinguishing uric acid and ammonium urate stones *in vivo*. This may optimize disease management and facilitate precision medicine in patients with urolithiasis.

Funding

This study was supported by the China Postdoctoral Science Foundation (Nos. 2021TQ0387, 2022M713625, and 2021M703709), the National Natural Science Foundation of China (Nos. 82203188 and 81825016), Guangdong Provincial Clinical Research Center for Urological Diseases (No. 2020B1111170006), and the Guangdong Basic and Applied Basic Research Foundation (No. 2020A1515111119).

Conflicts of interest

None.

Data availability statement

The data that support the findings of this study are available from the corresponding author on reasonable request.

References

1. De Coninck V, Antonelli J, Chew B, Patterson JM, Skolarikos A, Bultitude M. Medical expulsive therapy for urinary stones: Future trends and knowledge gaps. Eur Urol 2019;76:658–666. doi: 10.1016/j.eururo.2019.07.053.
2. Thongprayoon C, Krambeck AE, Rule AD. Determining the true burden of kidney stone disease. Nat Rev Nephrol 2020;16:736–746. doi: 10.1038/s41581-020-0320-7.
3. Qian X, Wan J, Xu J, Liu C, Zhong M, Zhang J, *et al*. Epidemiological trends of urolithiasis at the global, regional, and national levels: A population-based study. Int J Clin Pract 2022; 2022:6807203. doi: 10.1155/2022/6807203.
4. Rule AD, Lieske JC, Pais VM Jr. Management of kidney stones in 2020. JAMA 2020;323:1961–1962. doi: 10.1001/jama.2020.0662.
5. Türk C, Petřík A, Sarica K, Seitz C, Skolarikos A, Straub M, *et al*. EAU guidelines on interventional treatment for urolithiasis. Eur Urol 2016;69:475–482. doi: 10.1016/j.eururo.2015.07.041.
6. Miller AW, Choy D, Penniston KL, Lange D. Inhibition of urinary stone disease by a multi-species bacterial network ensures healthy oxalate homeostasis. Kidney Int 2019;96:180–188. doi: 10.1016/j.kint.2019.02.012.
7. Lu GL, Wang XJ, Huang BX, Zhao Y, Tu WC, Jin XW, *et al*. Comparison of mini-percutaneous nephrolithotomy and retroperitoneal laparoscopic ureterolithotomy for treatment of impacted proximal ureteral stones greater than 15 mm. Chin Med J 2021;134:1209–1214. doi: 10.1097/CM9.0000000000001417.
8. Türk C, Petřík A, Sarica K, Seitz C, Skolarikos A, Straub M, *et al*. EAU guidelines on diagnosis and conservative management of urolithiasis. Eur Urol 2016;69:468–474. doi: 10.1016/j.eururo.2015.07.040.
9. Pearle MS, Goldfarb DS, Assimos DG, Curhan G, Denu-Ciocca CJ, Matlaga BR, *et al*. Medical management of kidney stones: AUA guideline. J Urol 2014;192:316–324. doi: 10.1016/j.juro.2014.05.006.
10. Nourian A, Ghiraldi E, Friedlander JI. Dual-energy CT for urinary stone evaluation. Curr Urol Rep 2020;22:1. doi: 10.1007/s11934-020-01019-5.
11. Ilyas M, Dev G, Gupta A, Bhat TA, Sharma S. Dual-energy computed tomography: A reliable and established tool for in vivo differentiation of uric acid from nonuric acid renal Stones. Niger Postgrad Med J 2018;25:52–59. doi: 10.4103/npmj.npmj_24_18.
12. McGrath TA, Frank RA, Schieda N, Blew B, Salameh JP, Bossuyt PMM, *et al*. Diagnostic accuracy of dual-energy computed tomography (DECT) to differentiate uric acid from non-uric acid calculi: Systematic review and meta-analysis. Eur Radiol 2020;30:2791–2801. doi: 10.1007/s00330-019-06559-0.
13. Chou YH, Huang CN, Li WM, Huang SP, Wu WJ, Tsai CC, *et al*. Clinical study of ammonium acid urate urolithiasis. Kaohsiung J Med Sci 2012;28:259–264. doi: 10.1016/j.kjms.2011.11.004.
14. Lomas DJ, Jaeger CD, Krambeck AE. Profile of the ammonium acid urate stone former based on a large contemporary cohort. Urology 2017;102:43–47. doi: 10.1016/j.urology.2016.10.027.
15. Pichette V, Bonnardeaux A, Cardinal J, Houde M, Nolin L, Boucher A, *et al*. Ammonium acid urate crystal formation in adult North American stone-formers. Am J Kidney Dis 1997;30:237–242. doi: 10.1016/s0272-6386(97)90058-5.
16. Kuruma H, Arakawa T, Kubo S, Hyodo T, Matsumoto K, Satoh T, *et al*. Ammonium acid urate urolithiasis in Japan. Int J Urol 2006;13:498–501. doi: 10.1111/j.1442-2042.2006.01348.x.
17. Balla AA, Salah AM, Khattab AH, Kambal A, Bongartz D, Hoppe B, *et al*. Mineral composition of renal stones from the Sudan. Urol Int 1998;61:154–156. doi: 10.1159/000030312.
18. Xu W, Guo SL, Zhang SX. Chemical composition of upper urinary tract claculi: An analysis in 549 cases (in Chinese). J Wannan Med Coll 2014;33:131–133. doi: 10.3969/j.issn.1002-0217.2014.02.012.
19. Fan Y, Yuan GY, Wang YD, Xin YP, He K, Shao HG, *et al*. Analysis of the composition of upper urinary tract calculi and the prevention guideline of urinary tract calculi in Mianyang (in Chinese). Sichuan Med J 2016;37:1099–1102. doi: 10.16252/j.cnki.issn1004-0501-2016. 10. 010.
20. Zafar MN, Ayub S, Tanwri H, Naqvi SAA, Rizvi SAH. Composition of urinary calculi in infants: A report from an endemic country. Urolithiasis 2018;46:445–452. doi: 10.1007/s00240-017-1010-1.
21. Aggour A, Ziada AM, AbdelHamid AZ, AbdelRahman S, Morsi A. Metabolic stone composition in Egyptian children. J Pediatr Urol 2009;5:132–135. doi: 10.1016/j.jpurol.2008.11.002.
22. Kamoun A, Daudon M, Abdelmoula J, Hamzaoui M, Chaouachi B, Houissa T, *et al*. Urolithiasis in Tunisian children: A study of 120 cases based on stone composition. Pediatr Nephrol 1999;13:920–925; discussion 926. doi: 10.1007/s004670050728.
23. Kerrmu A, Guo F, Wumaner A, Wumaier D, Wang Q. Characteristics of urinary stone composition in Uyghur pediatric patients with urolithiasis (in Chinese). Int J Urol Nephrol 2014;34:837–840. doi: 10.3760/cma.j.issn.1673-4416.2014.06.018.
24. Sakhaee K, Adams-Huet B, Moe OW, Pak CY. Pathophysiologic basis for normouricosuric uric acid nephrolithiasis. Kidney Int 2002;62:971–979. doi: 10.1046/j.1523-1755.2002.00508.x.
25. Espinosa-Ortiz EJ, Eisner BH, Lange D, Gerlach R. Current insights into the mechanisms and management of infection stones. Nat Rev Urol 2019;16:35–53. doi: 10.1038/s41585-018-0120-z.
26. Miano R, Germani S, Vespasiani G. Stones and urinary tract infections. Urol Int 2007;79(Suppl 1):32–36. doi: 10.1159/000104439.
27. Bowyer RC, McCulloch RK, Brockis JG, Ryan GD. Factors affecting the solubility of ammonium acid urate. Clin Chim Acta 1979;95:17–22. doi: 10.1016/0009-8981(79)90331-0.
28. Klohn M, Bolle JF, Reverdin NP, Susini A, Baud CA, Graber P. Ammonium urate urinary stones. Urol Res 1986;14:315–318. doi: 10.1007/BF00262382.
29. Flannigan R, Choy WH, Chew B, Lange D. Renal struvite stones – Pathogenesis, microbiology, and management strategies. Nat Rev Urol 2014;11:333–341. doi: 10.1038/nrurol.2014.99.
30. Koras O, Bozkurt IH, Yonguc T, Degirmenci T, Arslan B, Gunlusoy B, *et al*. Risk factors for postoperative infectious

complications following percutaneous nephrolithotomy: A prospective clinical study. Urolithiasis 2015;43:55–60. doi: 10.1007/s00240-014-0730-8.
31. Skolarikos A, Straub M, Knoll T, Sarica K, Seitz C, Petřík A, *et al*. Metabolic evaluation and recurrence prevention for urinary stone patients: EAU guidelines. Eur Urol 2015;67:750–763. doi: 10.1016/j.eururo.2014.10.029.
32. Zheng X, Liu Y, Li M, Wang Q, Song B. Dual-energy computed tomography for characterizing urinary calcified calculi and uric acid calculi: A meta-analysis. Eur J Radiol 2016;85:1843–1848. doi: 10.1016/j.ejrad.2016.08.013.
33. Lambin P, Leijenaar RTH, Deist TM, Peerlings J, de Jong EEC, van Timmeren J, *et al*. Radiomics: The bridge between medical imaging and personalized medicine. Nat Rev Clin Oncol 2017;14:749–762. doi: 10.1038/nrclinonc.2017.141.
34. Bi WL, Hosny A, Schabath MB, Giger ML, Birkbak NJ, Mehrtash A, *et al*. Artificial intelligence in cancer imaging: Clinical challenges and applications. CA Cancer J Clin 2019;69:127–157. doi: 10.3322/caac.21552.
35. Li X, Pan Z, Wang X, Hu T, Ye W, Jiang D, *et al*. Prognostic nomogram incorporating radiological features for predicting overall survival in patients with AIDS-related non-Hodgkin lymphoma. Chin Med J 2022;135:70–78. doi: 10.1097/CM9.0000000000001785.
36. Zheng J, Yu H, Batur J, Shi Z, Tuerxun A, Abulajiang A, *et al*. A multicenter study to develop a non-invasive radiomic model to identify urinary infection stone in vivo using machine-learning. Kidney Int 2021;100:870–880. doi: 10.1016/j.kint.2021.05.031.
37. Babyak MA. What you see may not be what you get: A brief, nontechnical introduction to overfitting in regression-type models. Psychosom Med 2004;66:411–421. doi: 10.1097/01.psy.0000127692.23278.a9.
38. van Griethuysen JJM, Fedorov A, Parmar C, Hosny A, Aucoin N, Narayan V, *et al*. Computational radiomics system to decode the radiographic phenotype. Cancer Res 2017;77:e104–e107. doi: 10.1158/0008-5472.CAN-17-0339.
39. Zheng J, Kong J, Wu S, Li Y, Cai J, Yu H, *et al*. Development of a noninvasive tool to preoperatively evaluate the muscular invasiveness of bladder cancer using a radiomics approach. Cancer 2019;125:4388–4398. doi: 10.1002/cncr.32490.
40. Han K, Song K, Choi BW. How to develop, validate, and compare clinical prediction models involving radiological parameters: Study design and statistical methods. Korean J Radiol 2016;17:339–350. doi: 10.3348/kjr.2016.17.3.339.
41. Kramer AA, Zimmerman JE. Assessing the calibration of mortality benchmarks in critical care: The Hosmer-Lemeshow test revisited. Crit Care Med 2007;35:2052–2056. doi: 10.1097/01.CCM.0000275267.64078.B0.
42. Vickers AJ, Elkin EB. Decision curve analysis: A novel method for evaluating prediction models. Med Decis Making 2006;26:565–574. doi: 10.1177/0272989X06295361.
43. Pencina MJ, D'Agostino RB, D'Agostino RB, Vasan RS. Evaluating the added predictive ability of a new marker: From area under the ROC curve to reclassification and beyond. Stat Med 2008;27:157–172; discussion 207–112. doi: 10.1002/sim.2929.
44. Xia TH, Tan M, Li JH, Wang JJ, Wu QQ, Kong DX. Establish a normal fetal lung gestational age grading model and explore the potential value of deep learning algorithms in fetal lung maturity evaluation. Chin Med J 2021;134:1828–1837. doi: 10.1097/CM9.0000000000001547.

How to cite this article: Zheng JJ, Zhang J, Cai JH, Yao YH, Lu SH, Wu Z, Cai ZX, Tuerxun A, Batur J, Huang J, Kong JQ, Lin TX. Development of a radiomics model to discriminate ammonium urate stones from uric acid stones *in vivo*: A remedy for the diagnostic pitfall of dual-energy computed tomography. Chin Med J 2024;137:1095–1104. doi: 10.1097/CM9.0000000000002866